Estimating the structure of small dynamical networks from the state time evolution of one node

Raffaele Autariello,[1,3] Rhonda Dzakpasu,[2] and Francesco Sorrentino[1,*]

[1]*Department of Mechanical Engineering, University of New Mexico, Albuquerque, New Mexico 87131, USA*

[2]*Department of Physics, Georgetown University, Department of Pharmacology and Physiology, Georgetown University Medical Center, Washington, DC 20057, USA*

[3]*Dipartimento per le Tecnologie, Università degli studi di Napoli Parthenope, 80143 Napoli, Italy*

(Received 30 August 2012; revised manuscript received 12 November 2012; published 25 January 2013)

We consider small dynamical networks of coupled oscillators for which the network topology is unknown and try to use partial knowledge of the oscillators' dynamics to estimate both the network couplings and the states of the nodes. We focus on the case where the state time evolution from only one oscillator is available. We propose an adaptive strategy that uses synchronization between the true network and a replica network in order to estimate both the couplings and the states. The adaptive scheme is tested with several modules of coupled oscillators. We consider the effects of small mismatches in the parameters of the individual oscillators and we propose an alternative version of the strategy that is suitable to handle noise in the received signal.

DOI: 10.1103/PhysRevE.87.012915 PACS number(s): 05.45.Xt

I. INTRODUCTION

In this paper our objective is to identify the temporal structure of small networks, i.e., "modules," of coupled oscillators. We present an approach to estimating the strengths of couplings between the oscillators, as well as their states, while having limited knowledge about their dynamics. In particular, we proceed under the assumption that the state time evolution of only one node is available and we seek to use this information to estimate all of the unknown coupling strengths and states. Our approach is based on coupling an unknown true network to a replica network whose internal parameters can be adaptively evolved and trying to synchronize the two. Recent work has shown that synchronization can be used as a powerful tool to identify the dynamical equations of unknown systems [1–7]. Along the same lines, a Bayesian approach has been proposed in Refs. [8,9]. In contrast with previous studies, the strategy developed in this paper uses knowledge of the state time evolution of only one node. With only this available information, we show that, under certain conditions, it is possible to reconstruct all of the states of the nodes as well as all of the unknown connection strengths of an unknown network. The approach that we propose may be needed when direct access to several nodes is limited. Moreover, when the couplings are time varying, our strategy can be implemented to reconstruct the connections as they change over time. Thus our analysis applies to static networks but also more generally to dynamic networks for which the strengths of the connections evolve with time.

Our proposed problem is relevant to several fields. For example, in computer networks and power grids, variations in the connectivity of the network may signify the presence of faults [10]. In consensus and formation control problems [11,12], the strength of the connections typically varies in time. As a result, the ability to estimate these strengths is crucial in order to maintain connectivity within the network. In biological networks, such as genetic or neuronal networks, an important problem is that of reconstructing the network architecture and the time evolution of the connections from existing data. For these applications, a typical limitation is the cost and the possibility of accessing the states of the individual nodes. The network inference problem and its application to the genome [13–17] has received significative attention over the past decade. References [18,19] review and compare the more popular existing approaches. For gene expression assayed using microarrays, it is possible that hybridization of specific mRNA fragments is facilitated within certain sequences in the probes, so that certain genes are more easily detected than others [20,21]. Connectivity between neuronal cells remains a holy grail in neuroscience but, due to the current state of the art, only the wiring diagram of the nervous system of the nematode, *Caenorhabditis elegans*, with 302 neurons, has been fully elucidated [22]. However, knowledge of static connectivity tomographs is not sufficient to understand the function or complex computations of a given neural circuit. This is because the brain is a dynamical system and it is both the existence of a connection as well as its dynamical state that is required for neural communication.

It has been theoretically explored in Refs. [23,24] and experimentally tested in Ref. [25] that a sensor network can be realized by using a set of chaotic oscillators communicating via a wireless protocol. In the approach discussed in Refs. [23–25], each individual node needs to independently implement an adaptive strategy in order to maintain synchronization with the others and to be able to sense changes in the surrounding environment. An alternative approach has been proposed in [26] where an adaptive strategy is implemented to estimate the distance (i.e., the communication delay) between two coupled mobile platforms. An open question is whether similar strategies could be of use in the case where limited dynamical information is available about one or few of the network nodes. This is particularly relevant to neural systems since access is limited to a small subset of neurons in any neural circuit. Therefore, in this study, we discuss the applicability of our method to small modules of neuronal oscillators as a first step in an application to neural circuits (see Sec. VI).

In all of the above applications, it is important to be able to estimate the state of the network, i.e., the existence of connections between any pair of nodes, and their time

*Corresponding author: fsorrent@unm.edu

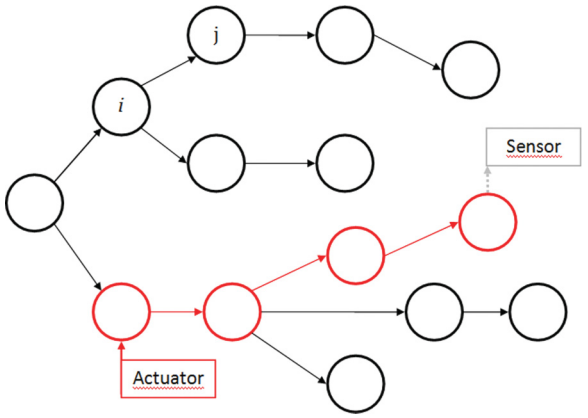

FIG. 1. (Color online) The figure shows a network characterized by a tree-like structure. We are able to control one node in the network and to sense the activity from a node downstream. The path of connections from the actuator to the sensor is highlighted in red (shown in dark gray). We show that our technique will be able to estimate connection strengths along this path.

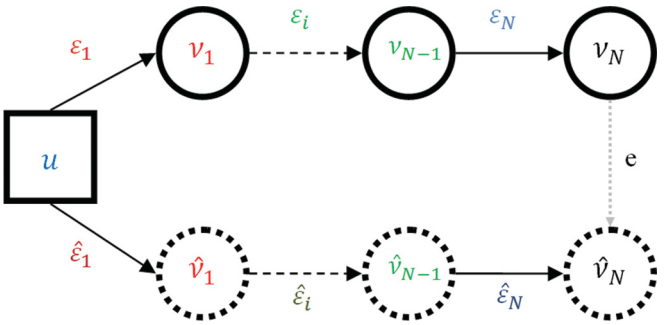

FIG. 2. (Color online) The top part of the figure shows a unidirectional chain of N coupled oscillators and the bottom part a replica chain (whose nodes are represented as dotted circles). The first oscillators of the real and replica chains are forced by the same input signal. A sensor is placed on the N^{th} oscillator of the original chain. The gray dotted line represents knowledge of the output time evolution of the N^{th} node that will be used by the adaptive strategy. The goal of the adaptive strategy is to synchronize the original and the replica chain by adapting the coupling strengths $\hat{\epsilon}_i$ of the replica until they converge onto the true ϵ_i.

evolution. The goal of the present paper is to provide a framework within which we demonstrate the possibility to infer the structure of a dynamical network, even when information about only one node is available. While a broad literature exists on estimating the topology of an unknown network from knowledge about the state time evolution of all of its nodes [27–33], to the best of our knowledge, the problem where only one node can be sensed has not been addressed. Keeping in mind the challenges in solving this problem for the case of networks of arbitrary size and complexity, we show that a solution exists for small networks formed of one or more (coupled) unidirectional chains.

The general problem discussed in this paper is illustrated in Fig. 1. We consider an arbitrary large complex network of coupled nodes. Each node in the figure is a dynamical system (an oscillator) and an arrow connects $i \to j$ if the dynamics of node i affects that of node j. Two of the nodes are chosen to be the source and the destination of a given path. An actuator is placed on the source node and a detector on the destination node. The path of connections from the actuator to the sensor is highlighted in red in Fig. 1. Our proposed goal is to be able to estimate the states of the nodes along the path from the source to the destination and the strengths of the couplings along that path. Different paths might be estimated by moving the position of the sensor and of the actuator over the network, with this type of approach being possibly easier to implement than trying to estimate the whole structure of the network at once. Note also that the treelike structure might be induced by the presence of the actuator if there is sufficient force exerted. For example, we propose that the scheme in Fig. 1 could be implemented for a sensor network where, by forcing one node and by recording the output of another node, the temporal evolution of the set of connections between the two can be reconstructed.

II. MODEL AND ADAPTIVE STRATEGY

As a first example of interest, we consider a chain of unidirectionally coupled oscillators. Chains of oscillators can describe many processes in nature, e.g., the undulatory locomotion of fish such as the lamprey or dogfish, peristalsis in the vascular and intestinal smooth muscles, communication of fireflies, and synchronization of emerging oscillations in a particular pathway of sensory processing in the cortex (see reviews in Refs. [34–36]).

This problem is represented in Fig. 2, where a chain of N unidirectionally coupled oscillators is shown. The first oscillator is forced by the input u^k, while the output of the N^{th} oscillator at the end of the chain is sensed.

The dynamics of a chain of unidirectionally coupled oscillators can be described by the following set of equations:

$$v_1^{k+1} = F\left(v_1^k\right) + \epsilon_1^k u^k, \tag{1a}$$

$$v_i^{k+1} = F\left(v_i^k\right) + \epsilon_i^k G\left(v_{i-1}^k\right), \quad i = 2, \ldots, N, \tag{1b}$$

where v_i^k is the n-dimensional state of node i at time k, $F : R^n \to R^n$ describes the dynamics of an uncoupled system, u^k is a driving signal, ϵ_i^k is the strength of the coupling from node $(i-1)$ to node i, $i = 2, \ldots, N$, ϵ_1^k is the coupling strength of the signal driving node 1, and $G : R^n \to R$ is a scalar output function.

In order to be able to identify the unknown couplings, we introduce a replica chain with coupling strengths that can be adaptively modified and we seek to synchronize this with the true chain. The equations for the replica network are the following:

$$\hat{v}_1^{k+1} = F\left(\hat{v}_1^k\right) + \hat{\epsilon}_1^k u^k, \tag{2a}$$

$$\hat{v}_i^{k+1} = F\left(\hat{v}_i^k\right) + \hat{\epsilon}_i^k G\left(\hat{v}_{i-1}^k\right), \quad i = 2, \ldots, N, \tag{2b}$$

where $\hat{v}_i^k$ is the n-dimensional state of node i at time k, and $\hat{\epsilon}_i$, $i = 1, \ldots, N$ are estimates at the replica system of the true couplings ϵ_i, $i = 1, \ldots, N$. In Fig. 2, the nodes of the replica chain are represented as dotted circles. We assume that the only available information about the dynamics of the original network is the state time evolution of the N^{th} node. The gray dotted line represents this information that will be used by our adaptive strategy in order to estimate the ϵ_i.

We observe that for $\hat{\epsilon}_i = \epsilon_i$, $i = 1,\ldots,N$, the replica chain may synchronize to the original chain by virtue of the common driving input, u^k. This means that $|\nu_i^k - \hat{\nu}_i^k| \to 0$, for $i = 1,\ldots,N$. Hence, we seek to use synchronization between the original and the replica system to dynamically estimate the unknown ϵ_i, $i = 1,\ldots,N$. In particular, in what follows we modulate the coupling strengths of the replica network until they converge onto those of the original network and synchronization is achieved.

We note here that the ϵ_i in Eq. (1a) to be estimated are functions of the time k. However, one of our underlying assumptions is that the ϵ_i^k evolve on a time scale T_ϵ that is much longer than the time scale T_ν on which an individual system evolves, i.e.,

$$T_\nu \ll T_\epsilon. \tag{3}$$

Our adaptive strategy then can be implemented over a time scale over which the unknown ϵ_i^k are nearly constant. The specificity of our approach lies in the fact that knowledge about the state time evolution of only one system is exploited to estimate all of the couplings in the chain, i.e., we attempt to estimate ϵ_i, $i = 1,\ldots,N$ based on the sole knowledge of ν_N^k. In order to do that we introduce an appropriately defined potential,

$$\psi^k = \left[G\left(\nu_N^k\right) - G\left(\hat{\nu}_N^k\right)\right]^2, \tag{4}$$

under the assumption that the quantity

$$I^k \equiv G\left(\nu_N^k\right) \tag{5}$$

is the only available information from the original network. We see that ψ^k is zero when $\hat{\nu}_i^k = \nu_i^k$ and $\hat{\epsilon}_i^k = \epsilon_i^k$, $i = 1,\ldots,N$. Hence, in what follows we seek to minimize the potential (4). Our strategy consists of evolving the $\hat{\epsilon}_i^k$ $i = 1,\ldots,N$ in order to minimize the potential. To this aim, we introduce the following gradient descent relations,

$$\hat{\epsilon}_i^{k+1} = \hat{\epsilon}_i^k - \gamma_i \frac{\partial \psi^{k'}}{\partial \hat{\epsilon}_i} = \hat{\epsilon}_i^k + 2\gamma_i e^{k'} DG \frac{\partial \hat{\nu}_N^{k'}}{\partial \hat{\epsilon}_i}, \tag{6}$$

$i = 1,\ldots,N$, where $e^k = [G(\nu_N^k) - G(\hat{\nu}_N^k)]$, DG is the Jacobian of the function G, and γ_i is a positive scalar. Note that Eq. (6) applies to the potential ψ being evaluated at a generic time k'. We proceed under the assumption that for k' close to k minimizing $\psi^{k'}$ is approximately the same as minimizing ψ^k. From Eq. (2) we see that

$$\hat{\nu}_i^{k+2} = F\left(\hat{\nu}_i^{k+1}\right) + \hat{\epsilon}_i G\left[F\left(\hat{\nu}_{i-1}^k\right) + \hat{\epsilon}_{i-1} G\left(\hat{\nu}_{i-2}^k\right)\right], \tag{7}$$

$i = 3,\ldots,N$ and for r being a positive integer, we have

$$\begin{aligned}\hat{\nu}_i^{k+r} = {} & F\left(\hat{\nu}_i^{k+r-1}\right) + \hat{\epsilon}_i G\left[F\left(\hat{\nu}_{i-1}^{k+r-2}\right)\right. \\ & \left. + \hat{\epsilon}_{i-1} G\left(\cdots + \hat{\epsilon}_{i-r+1} G\left(\hat{\nu}_{i-r}^k\right)\right)\right]\end{aligned} \tag{8}$$

$i = (r+1),\ldots,N$. We find that the most convenient way of implementing Eq. (6) is the following:

$$\begin{aligned}\hat{\epsilon}_i^{k+1} &= \hat{\epsilon}_i^k - \gamma_i \frac{\partial \psi^{(k+N-i+1)}}{\partial \hat{\epsilon}_i} = \hat{\epsilon}_i^k + 2\gamma_i e^{(k+N-i+1)} \frac{\partial \hat{\nu}_N^{(k+N-i+1)}}{\partial \hat{\epsilon}_i} \\ &= \hat{\epsilon}_i^k + 2\gamma_i e^{(k+N-i+1)} \left[\prod_{j=(i+1)}^{N} \hat{\epsilon}_j DG\right] G\left(\hat{\nu}_{i-1}^k\right).\end{aligned} \tag{9}$$

From the latter equation we note that in order to implement the adaptive strategy, knowledge of $e^{(k+N-i+1)}$ is required. Yet, for N not being too large and the individual error $e^{(k+N-i+1)}$ not evolving too fast, we can assume that $e^{(k+N-i+1)} \cong e^k$. Using this approximation, we get

$$\hat{\epsilon}_i^{k+1} \cong \hat{\epsilon}_i^k + 2\gamma_i e^k \left[\prod_{j=(i+1)}^{N} \hat{\epsilon}_j DG\right] G\left(\hat{\nu}_{i-1}^k\right). \tag{10}$$

A. Numerical experiment

We consider, first, a unidirectional chain of $N = 3$ coupled oscillators. To test our measure, we implement the neuronal model described in Refs. [37,38] as the function F, for which $n = 2$, $\nu^k = (x^k, y^k)^T$,

$$F(\nu^k) = \begin{cases} x_i^{k+1} = \left(x_i^k\right)^2 \exp^{(y_i^k - x_i^k)} + d \\ y_i^{k+1} = a y_i^k - b x_i^k + c \end{cases}. \tag{11}$$

This equation results in chaotic dynamics for the following choices of parameters: $a = 0.89$, $b = 0.18$, $c = 0.28$, and $d = 0.03$ [37]. We choose the function G to be

$$G(\nu^k) = \begin{bmatrix} 1 & 0 \\ 0 & 0 \end{bmatrix} \nu^k. \tag{12}$$

In our first experiment, we set the drive $u^k = 1 + \sin(0.06\pi k)$ and the initial conditions for x_i^k, y_i^k and $\hat{x}_i^k, \hat{y}_i^k$ to be random numbers drawn from a uniform distribution in the interval $[0,1]$, $i = 1,\ldots,N$. The initial guesses $\hat{\epsilon}_i^0$ are random numbers drawn from a uniform distribution in the interval [0.10,0.40]. The true ϵ_i are time-varying functions,

$$\epsilon_i^k = \bar{\epsilon}_i + 0.05 \sin(4 \times 10^{-6} \pi k), \tag{13}$$

where $\bar{\epsilon}_1 = 0.3$, $\bar{\epsilon}_2 = 0.2$, and $\bar{\epsilon}_3 = 0.4$.

The results of our numerical simulations are shown in Figs. 3 and 4. Figure 3 shows $\hat{x}_2^k$ versus x_2^k at the beginning and at the end of the run. As can be seen, for large-enough k, x_2 and $\hat{x}_2$ synchronize. Though not explicitly shown, all of the $\hat{x}_i^k$ converge on the time evolutions of the true x_i^k, $i = 1,\ldots,N$. Figure 4 shows $\hat{\epsilon}_i^k$ versus ϵ_i^k for $i = 1,\ldots,3$, with all of our estimates tracking the time evolution of the true couplings.

In our second experiment, we set the drive $u^k = x^k$, where x^k is obtained by iterating the equation for a neuron model [37,38],

$$\begin{aligned} x^{k+1} &= (x^k)^2 \exp^{(y^k - x^k)} + 0.03 \\ y^{k+1} &= 0.89 y^k - 0.18 x^k + 0.28. \end{aligned} \tag{14}$$

The initial conditions for x_i^k, y_i^k and $\hat{x}_i^k$, $\hat{y}_i^k$ are random numbers drawn from a uniform distribution in the interval $[0,1]$, $i = 1,\ldots,N$. We set the initial guesses $\hat{\epsilon}_i^0$ to be random numbers drawn from a uniform distribution in the interval [0.10,0.50]. The true ϵ_i are time-varying functions,

$$\epsilon_i^k = \bar{\epsilon}_i + 0.05 \sin(4 \times 10^{-5} \pi k), \tag{15}$$

where $\bar{\epsilon}_1 = 0.3$, $\bar{\epsilon}_2 = 0.2$, and $\bar{\epsilon}_3 = 0.4$. We set $\gamma_i = 10^{-3}$, $i = 1,\ldots,N$.

The results of our numerical simulations are shown in Figs. 5 and 6. Figure 5 shows $\hat{x}_2^k$ versus x_2^k at the beginning

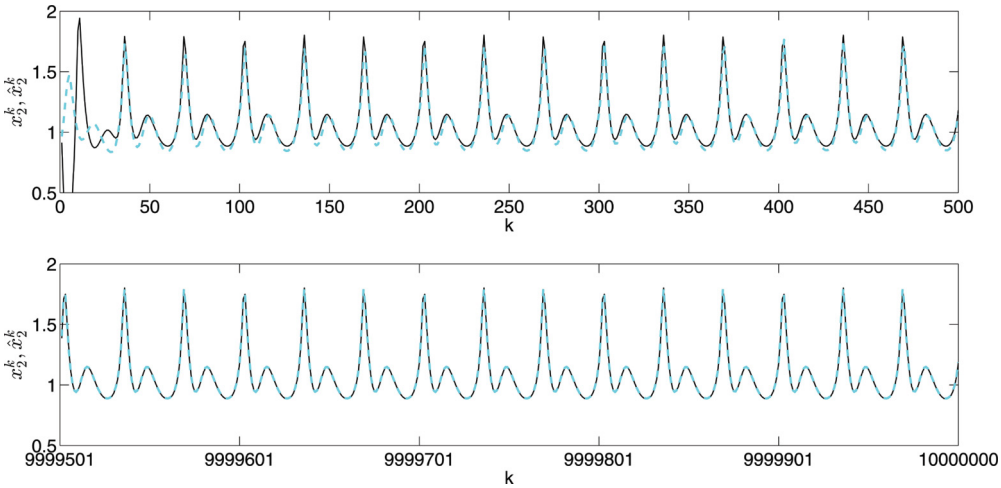

FIG. 3. (Color online) Top figure: x_2^k (solid line) and $\hat{x}_2^k$ (dashed line) at the beginning of the simulation. Bottom figure: x_2^k (solid line) and $\hat{x}_2^k$ (dashed line) at the end of the simulation.

and at the end of the run. As can be seen for large-enough k, x_2 and $\hat{x}_2$ synchronize. Though not explicitly shown, all of the $\hat{x}_i^k$ converge on the time evolutions of the true x_i^k, $i = 1, \ldots, N$. Figure 6 shows $\hat{\epsilon}_i^k$ versus ϵ_i^k for $i = 1, \ldots, 3$, with all of our estimates tracking the time evolution of the true couplings.

1. Dependence on N

We tested our adaptive strategy for unidirectional chains of increasing length N. For each run we chose the ϵ_i to be constant over the time of the simulation and equal to N equally spaced numbers in the interval [0.2,0.5]. The initial conditions for $\hat{\epsilon}_i$ were chosen as $\hat{\epsilon}_i^0 = \epsilon_i + \eta_i$, where η_i is a random number drawn from a uniform distribution in the range $[-0.05, +0.05]$. We ran the simulations for a long time from $k = 0$ to $k = 5 \times 10^6$ and recorded the final normalized estimation error,

$$\Delta = ((k_2 - k_1)N)^{-1} \sum_{k=k_1}^{k_2} \sum_{i=1}^{N} \frac{|\epsilon_i - \hat{\epsilon}_i^k|}{|\epsilon_i|}, \qquad (16)$$

where we set $k_1 = 4.5 \times 10^6$ and $k_2 = 5 \times 10^6$. For all our simulations we chose $\gamma_1 = \cdots = \gamma_N = 10^{-4}$. Figure 7 shows $\Delta(N)$ versus $N = 2,3, \ldots, 6$. As can be seen, the performance of our adaptive strategy degrades as the length of the chain N increases.

III. A PARALLEL CONFIGURATION

As a second example, we consider the network layout represented in Fig. 8, where the actuator is connected to the sensor through two or more independent unidirectional paths. As can be seen from the figure, a common driver independently forces two unidirectional chains of oscillators which come together in the sensed node. In this example, four connections will have to be estimated: ϵ_{01}, ϵ_{02}, ϵ_{13}, and ϵ_{23}.

The dynamics of the network configuration in Fig. 8 can be described by the following set of equations:

$$v_i^{k+1} = F(v_i^k) + \epsilon_{0i}^k u^k, \qquad i = 1,2. \qquad (17a)$$

$$v_3^{k+1} = F(v_3^k) + [\epsilon_{13}^k G(v_1^k) + \epsilon_{23}^k G(v_2^k)]. \qquad (17b)$$

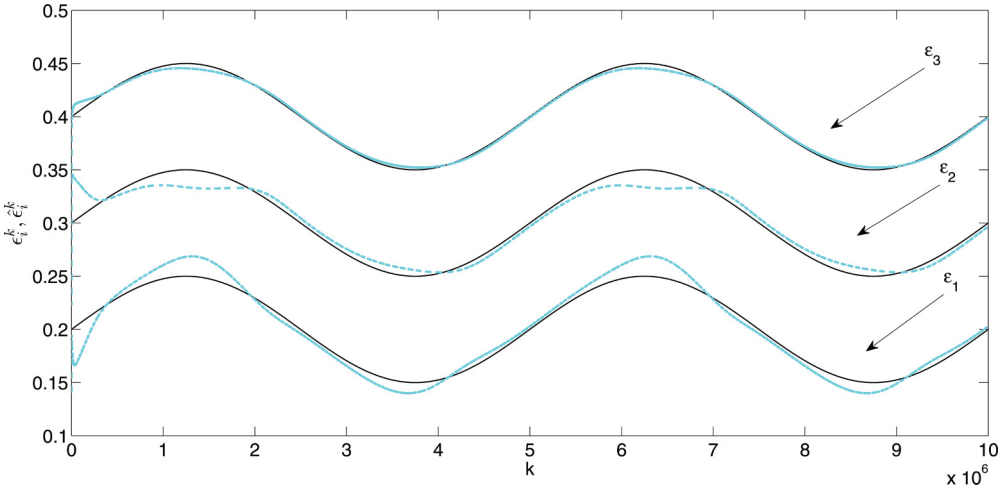

FIG. 4. (Color online) Time evolution of ϵ_i^k (solid lines) and of $\hat{\epsilon}_i^k$ (dashed lines).

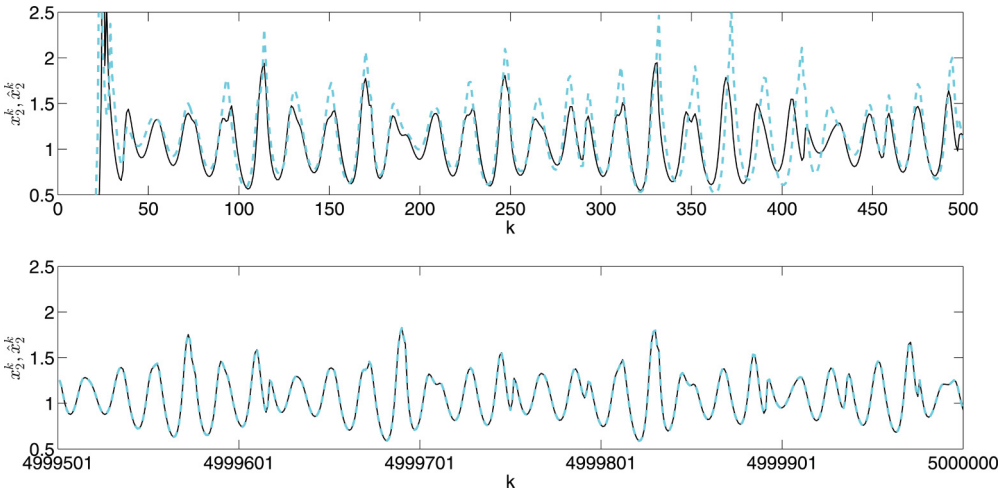

FIG. 5. (Color online) Top figure: x_2^k (solid line) and $\hat{x}_2^k$ (dashed line) at the beginning of the simulation. Bottom figure: x_2^k (solid line) and $\hat{x}_2^k$ (dashed line) at the end of the simulation.

The equations for the replica network are as follows:

$$\hat{v}_i^{k+1} = F\left(\hat{v}_i^k\right) + \hat{\epsilon}_{0i}^k u^k, \quad i = 1,2. \tag{18a}$$

$$\hat{v}_3^{k+1} = F\left(\hat{v}_3^k\right) + \left[\hat{\epsilon}_{13}^k G\left(\hat{v}_1^k\right) + \hat{\epsilon}_{23}^k G\left(\hat{v}_2^k\right)\right], \tag{18b}$$

where $\hat{v}_i^k$ is the n-dimensional state of node i at time k, and $\hat{\epsilon}_{ij}$ are estimates at the replica system of the true ϵ_{ij}. Following the same approach presented in Sec. II, we obtain the following adaptive strategy:

$$\hat{\epsilon}_{0i}^{k+1} \cong \hat{\epsilon}_{0i}^k + 2\gamma e^k DG\hat{\epsilon}_{i3}^k u^k, \quad i = 1,2, \tag{19a}$$

$$\hat{\epsilon}_{i3}^{k+1} \cong \hat{\epsilon}_{i3}^k + 2\gamma e^k G\left(\hat{v}_i^k\right), \quad i = 1,2. \tag{19b}$$

We set the initial conditions for x_i^k, y_i^k and $\hat{x}_i^k, \hat{y}_i^k$ to be random numbers drawn from a uniform distribution in the interval $[0,1]$, $i = 1,\ldots,N$. The initial guesses $\hat{\epsilon}_{ij}^0$ were chosen as $\hat{\epsilon}_{ij}^0 = \bar{\epsilon}_{ij} + \eta_{ij}$, where η_{ij} is a random number drawn from a uniform distribution in the range $[-0.03, +0.03]$. The true ϵ_{ij} are time-varying functions,

$$\epsilon_{ij}^k = \bar{\epsilon}_{ij} + 0.05\sin(4 \times 10^{-6}\pi k), \tag{20}$$

where $\bar{\epsilon}_{01} = 0.3$, $\bar{\epsilon}_{02} = 0.2$, $\bar{\epsilon}_{13} = 0.5$, and $\bar{\epsilon}_{23} = 0.4$. We set $\gamma = 10^{-4}$.

The results of our numerical simulations are shown in Fig. 9, where the estimates $\hat{\epsilon}_{ij}^k$ are shown versus ϵ_{ij}^k for $(i,j) = (0,1),(0,2),(1,3),(2,3)$, with all of our estimates tracking the time evolution of the true couplings.

We note here that estimating the ϵ_{ij} corresponds to finding an estimate adjacency matrix $\hat{E} = \{\hat{\epsilon}_{ij}\}$, $i,j = 1,\ldots,N$ that approximates the true adjacency matrix $E = \{\epsilon_{ij}\}$. While for the example of the unidirectional chain there exists only one possible graph representation of the matrix E, for the parallel configuration considered in this section there are two: one for which the labeling of the nodes is the same in E as in $\hat{E}$ and one for which node $1 \to 2$ and node $2 \to 1$. Indeed, we sometimes observed in simulation that $\hat{\epsilon}_{01}$ converged on ϵ_{02}, $\hat{\epsilon}_{02}$ converged on ϵ_{01}, $\hat{\epsilon}_{13}$ converged on ϵ_{23}, and $\hat{\epsilon}_{23}$ converged on ϵ_{13} (not shown). We found this result satisfying

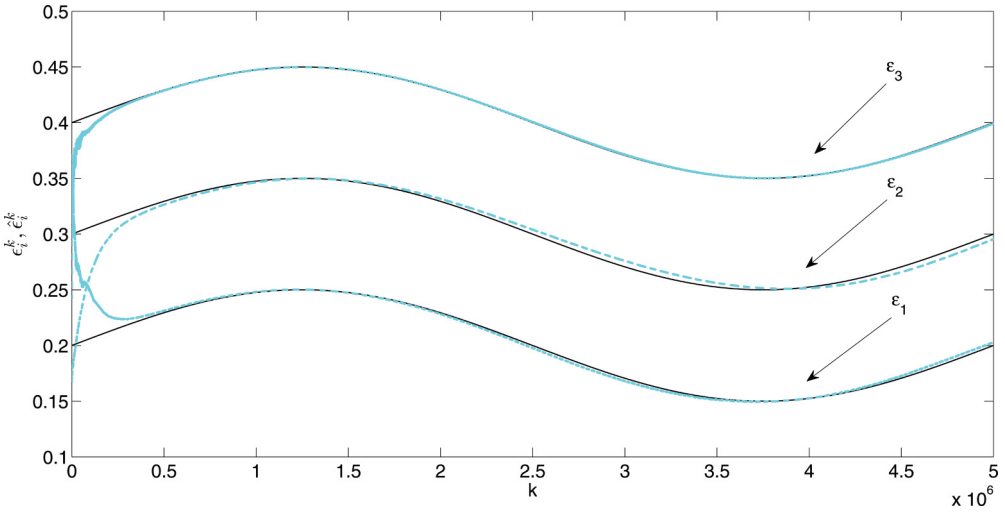

FIG. 6. (Color online) Time evolution of ϵ_i^k (solid lines) and of $\hat{\epsilon}_i^k$ (dashed lines), $i = 1,\ldots,N$.

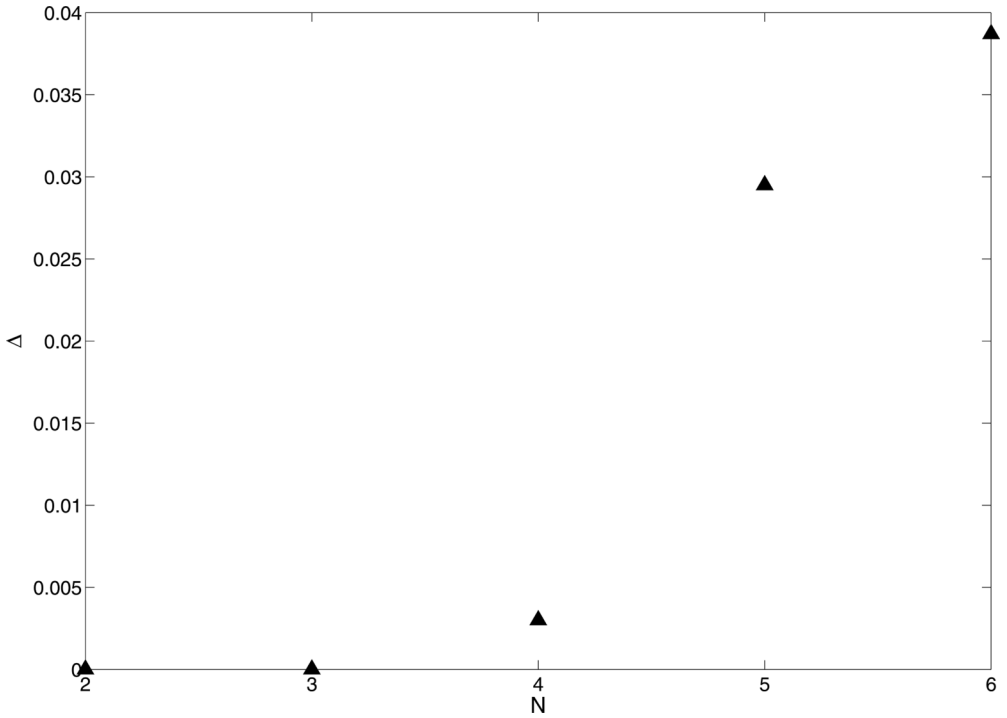

FIG. 7. We test the adaptive strategy for unidirectional chains of increasing length N. The figure shows the estimation error Δ defined in Eq. (16) versus N.

since our goal was to obtain a correct representation of the original matrix, independent of the labeling of the nodes. More generally, our aim could be recast as that of seeking a matrix $\hat{E}$ such that $\hat{E} = PEP$ where $P = \{p_{ij}\}$ is any permutation matrix with $p_{NN} = 1$.

A. A more complex configuration

We attempted to apply an approximate version of the adaptive strategy to a more complex configuration, in which the dynamics of the two chains in Fig. 8 are mutually coupled. In particular, we considered the case when two extra connections are added to the network layout in Fig. 8, namely one connection from node 1 to node 2 with associated strength ϵ_{12} and one connection from node 2 to node 1 with associated strength ϵ_{21}. The dynamics for such a network is described by the following set of equations:

$$v_i^{k+1} = F\left(v_i^k\right) + \epsilon_{0i}^k u^k + \epsilon_{ji}^k G\left(v_j^k\right), \quad i = 1,2, \tag{21a}$$
$$v_3^{k+1} = F\left(v_3^k\right) + \left[\epsilon_{13}^k G\left(v_1^k\right) + \epsilon_{23}^k G\left(v_2^k\right)\right], \tag{21b}$$

where the subscript $j = (3 - i)$. The equations for the replica network are as follows:

$$\hat{v}_i^{k+1} = F\left(\hat{v}_i^k\right) + \hat{\epsilon}_{0i}^k u^k + \hat{\epsilon}_{ji}^k G\left(\hat{v}_j^k\right), \quad i = 1,2, \tag{22a}$$
$$\hat{v}_3^{k+1} = F\left(\hat{v}_3^k\right) + \left[\hat{\epsilon}_{13}^k G\left(\hat{v}_1^k\right) + \hat{\epsilon}_{23}^k G\left(\hat{v}_2^k\right)\right], \tag{22b}$$

where again $j = (3 - i)$. For this case, there are six unknown coupling strengths: $\epsilon_{01}, \epsilon_{02}, \epsilon_{12}, \epsilon_{21}, \epsilon_{13}$, and ϵ_{23}. Following the same approach presented in Sec. II, we obtain an approximate version of the adaptive strategy:

$$\hat{\epsilon}_{0i}^{k+1} \cong \hat{\epsilon}_{0i}^k + 2\gamma e^k DG\hat{\epsilon}_{i3}^k u^k, \quad i = 1,2, \tag{23a}$$
$$\hat{\epsilon}_{i3}^{k+1} \cong \hat{\epsilon}_{i3}^k + 2\gamma e^k G\left(\hat{v}_i^k\right), \quad i = 1,2, \tag{23b}$$
$$\hat{\epsilon}_{ij}^{k+1} \cong \hat{\epsilon}_{ij}^k + 2\gamma e^k DG\hat{\epsilon}_{j3}^k G\left(\hat{v}_i^k\right), \quad i = 1,2, \quad j = (3 - i). \tag{23c}$$

We performed experiments similar to the one presented in the first part of Sec. III but we considered the presence of the other two couplings, ϵ_{12} and ϵ_{21}, which we attempted to estimate. For simplicity, we set the ϵ_{ij} to be constant over the time scale of the simulation. The results of this numerical experiment are described in Fig. 10, where we show that by iterating the adaptive strategy, the estimates $\hat{\epsilon}_{12}$ and $\hat{\epsilon}_{21}$ converge on the true values of ϵ_{12} and ϵ_{21}, respectively.

IV. EFFECTS OF NOISE ON THE ADAPTIVE STRATEGY

In this section we focus on the chain of unidirectionally coupled oscillators studied in Sec. II and we consider the presence of noise in the communication channel between the true and the replica chains. We assume additive noise and we replace the received signal I^k in (5) by

$$I^k = G\left(v_N^k\right) + r\sigma\rho^k, \tag{24}$$

where ρ^k is a zero-mean independent random number of unit variance drawn from a Gaussian distribution, σ is the numerically computed standard deviation of $G(v_N^k)$, and r is multiplicative factor.

To facilitate adaption when noise is present in the received signal, we propose an alternative formulation of our adaptive

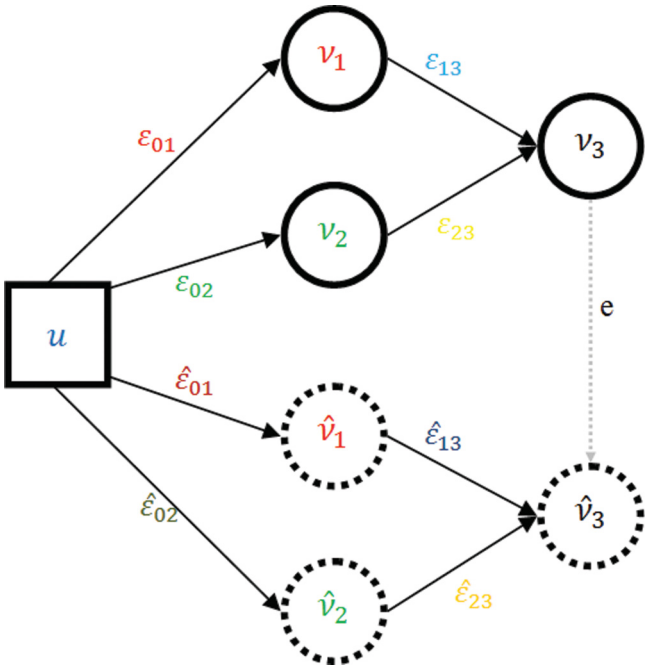

FIG. 8. (Color online) The top part of the figure shows a network of coupled oscillators in a parallel configuration, i.e., for which the actuator is connected to the sensor through two independent unidirectional paths. The bottom part of the figure shows a replica network (whose nodes are represented as dotted circles). The oscillators labeled 1 and 2 of the original and replica networks are forced by the same input signal. A sensor is placed on the third oscillator of the original network. The gray dotted line represents knowledge of the output time evolution of the third node that will be used by the adaptive strategy. The goal of the adaptive strategy is to synchronize the original and the replica network on the same time evolution by adapting the coupling strengths $\hat{\epsilon}_{ij}$ of the replica until they converge onto the original ϵ_{ij}.

strategy for which the potential (4) is replaced by

$$\langle \psi^k \rangle_z, \tag{25}$$

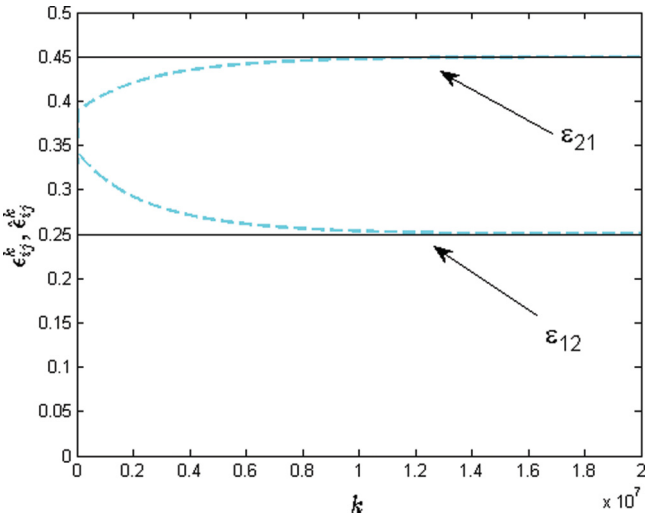

FIG. 10. (Color online) Time evolution of ϵ_{ij}^k, the assumed constant (solid lines), and their estimates $\hat{\epsilon}_{ij}^k$ (dashed lines).

where the symbol

$$\langle A^k \rangle_z = (1-z)\sum_{j=0}^{\infty} z^j A^{k-j} \tag{26}$$

and z is a smoothing factor that determines the temporal extent over which the averaging is performed. The time window over which this exponentially weighted moving averaging is performed is $(1-z)^{-1}$ samples. Note that based on the above definition, $\langle A^{k+1} \rangle_z = z\langle A^k \rangle_z + (1-z)A^k$.

We require $(1-z)^{-1}$ to be larger than T_ν, the characteristic time scale over which an uncoupled system evolves, and to be smaller than T_ϵ, the time scale over which the true couplings evolve, i.e.,

$$T_\nu < (1-z)^{-1} < T_\epsilon. \tag{27}$$

Note that $\langle \psi^k \rangle_z \geqslant 0$. Moreover, $\langle \psi^k \rangle_z = 0$ only if $\hat{\nu}_i^k = \nu_i^k$ and $\hat{\epsilon}_i = \epsilon_i$, $i = 1, \ldots, N$. Thus, in what follows we seek to minimize the potential (25). We introduce the following

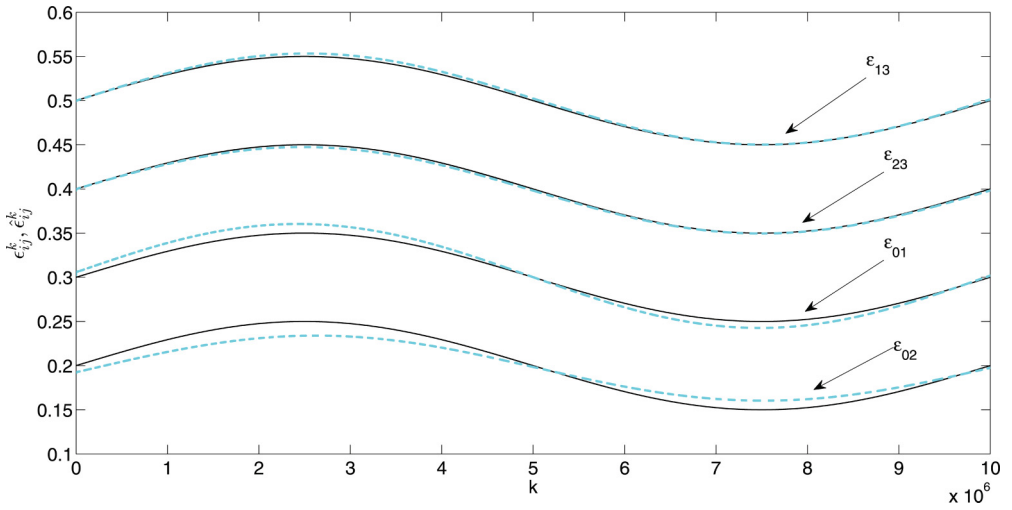

FIG. 9. (Color online) Time evolution of ϵ_{ij}^k (solid lines) and of $\hat{\epsilon}_{ij}^k$ (dashed lines).

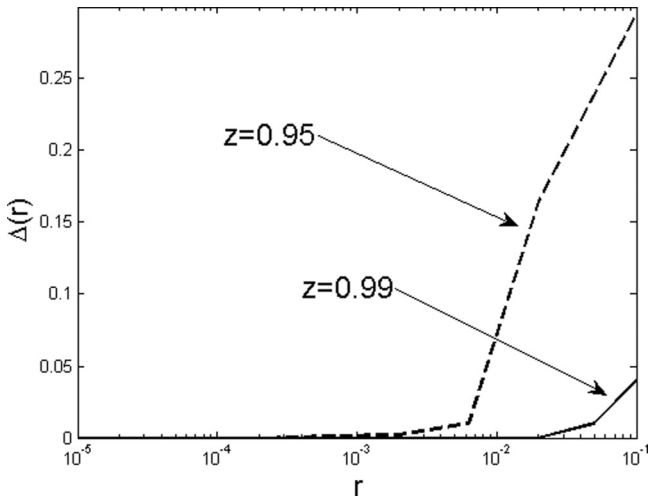

FIG. 11. Final estimation Δ versus r for both the cases of $z = 0.95$ and $z = 0.99$.

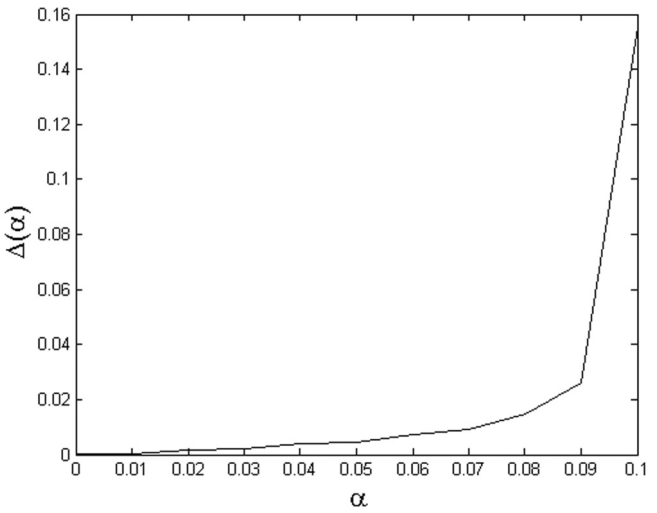

FIG. 12. Final estimation error Δ versus the parameter-mismatch coefficient α. Each point in the figure is an average over 20 different realizations of the estimation strategy.

gradient descent relations:

$$\hat{\epsilon}_i^{k+1} = \hat{\epsilon}_i^k - \gamma_i \frac{\partial}{\partial \hat{\epsilon}_i} \langle \psi^{k'} \rangle_z \tag{28}$$

$i = 1, \ldots, N$, $\gamma_i > 0$. With this modification, Eq. (10) for the evolution of the $\hat{\epsilon}_i$ is replaced by

$$\hat{\epsilon}_i^{k+1} = \hat{\epsilon}_i^k + 2\gamma_i \xi_i^k, \tag{29a}$$

$$\xi_i^{k+1} = z\xi_i^k + (1-z)e^k \left[\prod_{j=(N-i+1)}^{N} \hat{\epsilon}_j DG \right] G\left(\hat{v}_{N-1}^k\right), \tag{29b}$$

$i = 1, \ldots, N$. Figure 11 shows the performance of our adaptive strategy [Eqs. (1), (2), and (29)] as the noise coefficient r is increased. We set $N = 3$. For each run we choose the ϵ_i to be constant over the time of the simulation and equal to N equally spaced numbers in the interval [0.2,0.5]. We plot the final estimation error Δ versus r for both cases where $z = 0.95$ and $z = 0.99$. As can be seen, for r not being too large, the adaptive strategy is able to reconstruct all of the unknown couplings in the presence of noise.

V. ROBUSTNESS OF THE ADAPTIVE STRATEGY WITH RESPECT TO MODEL MISMATCHES

In this section, we test our strategy in the case that our model equations do not exactly match those characterizing the dynamics of the true network. In particular, we assume that the parameters for each individual neuron slightly deviate from the true ones. To this aim, we replace the set of equations (2) describing the replica network by the following set of equations:

$$\hat{v}_1^{k+1} = \tilde{F}\left(\hat{v}_1^k\right) + \hat{\epsilon}_1^k u^k, \tag{30a}$$

$$\hat{v}_i^{k+1} = \tilde{F}\left(\hat{v}_i^k\right) + \hat{\epsilon}_i^k G\left(\hat{v}_{i-1}^k\right), \quad i = 2, \ldots, N, \tag{30b}$$

where the function $\tilde{F}$ is an imperfect model of the true function F, i.e.,

$$\tilde{F}(v^k) = \begin{cases} x_i^{k+1} = \left(x_i^k\right)^2 \exp^{(y_i^k - x_i^k)} + d' \\ y_i^{k+1} = a' y_i^k - b' x_i^k + c' \end{cases}, \tag{31}$$

with parameters $a' = a(1+\beta_a)$, $b' = b(1+\beta_b)$, $c' = c(1+\beta_c)$, $d' = d(1+\beta_d)$, with $(\beta_a, \beta_b, \beta_c, \beta_d)$ being random numbers drawn from a Gaussian distribution with a 0 mean and standard deviation α.

Figure 12 shows the performance of our adaptive strategy, Eqs. (1), (10), and (30), as the parameter-mismatch coefficient α is increased. We set $N = 3$. For each run we choose ϵ_i to be constant over the time of the simulation and equal to N equally spaced numbers in the interval [0.2,0.5]. We plot the final estimation error $\Delta(\alpha)$, averaged over many realizations, versus α. Note that by increasing α, we introduce model mismatches in all of the parameters of all the oscillators in the chain. As can be seen, for α not being too large, the adaptive strategy is still able to provide good estimates of the unknown couplings in the presence of model mismatches.

VI. DISCUSSION: AN APPLICATION TO NEURONAL NETWORKS

In this section, we comment on the possible application of our technique to estimating synaptic strengths within small neuronal networks, which remains an outstanding problem in neuroscience. According to the current state of the art, experiments can be carried out to both sense and control single neurons [39,40]. However, the possibility of sensing multiple neurons is typically limited by technological constraints. We are particularly interested in the application of our adaptive strategy to neural systems as these circuits pose a unique challenge in the elucidation of connectivity. Not only is access to the circuit limited by technological constraints but the connectivity is an activity-dependent dynamical process.

In order to begin to link form with function within a neural system, knowledge about its connectivity pattern is the first important step. The field of connectomics involves the elucidation of the structural connectivity profile for a given neural system [41]. Imaging of the brain anatomy to obtain the architecture of this complex circuit will help to provide insights into behavior as well as identify loci of a particular neuropathology. Structural connectivity can span a wide spatial range with cell-to-cell connectivity maps comprising the microscopic scale and on the macroscopic scale, connectivity maps between assembles of neurons or between specific anatomical regions [42–45]. In particular, at the microscopic scale, connectivity between cells remains a holy grail in neuroscience but, due to the current state of the art, only the wiring diagram of the nervous system of the nematode *Caenorhabditis elegans*, with 302 neurons, has been fully elucidated [22].

However, knowledge of static connectivity tomographs is not sufficient to understand the function or complex computations of a given neural circuit. The brain is a dynamical system and it is both the existence of a connection as well as its dynamical state that is required for neural communication. This points out the importance of developing tools to detect and monitor the time evolution of the connectivity patterns between neurons. Measuring the strength of synapses and how they change over time is a necessary component of understanding neural function. This task is more challenging because complete knowledge of the dynamics of any given circuit is not known. Experimentally, assessing synaptic strength is typically performed using single electrodes, thereby placing a limit on the overall number of synapses that can be measured.

We find two main limitations to the possibility of applying our technique to neural networks: (i) in experiments, only approximate synchronization between a true neuron and a model neuron has been achieved and (ii) neural networks are typically characterized by a degree of complexity that is higher than that of the simple modules considered in this paper. While the first problem points out the importance of developing tools that are robust with respect to model uncertainties, the second problem suggests that our technique could be successfully applied to an *in vitro* network of cultured neurons synthetically coupled as in Ref. [46]. Our capability of estimating the parameters and the states of an experimental realization similar to that proposed in Ref. [46] would allow us to produce a proof-of-principle demonstration of the possibility of applying our technique to networks of neurons.

While the current state of our strategy is not ready for a practical implementation, we speculate that future analytical and computational refinement in conjunction with the testing of an experimental application will achieve this goal. A representative sensor-actuator system in the brain is the class of nociceptors, sensory neurons that respond to mechanical, chemical, and thermal stimulation, and their corresponding output neurons that adjust or modulate their dynamics in response to the sensor. Taking this as a model, we believe it is possible that a future realization would combine visual and dynamical techniques to improve the resolution needed to describe the dynamic network connectivity structure as well as to shed light on its time evolution.

VII. CONCLUSION

In this paper we considered small networks (modules) of coupled oscillators with the goal of estimating all of the unknown network couplings, using limited, i.e., localized, information on the state time evolution from only one oscillator.

We proposed an adaptive strategy that uses synchronization between an original true network and a replica network in order to estimate the couplings and the states of the oscillators. We tested our approach over different modules of coupled oscillators, including small unidirectional chains and a configuration of two (coupled) chains in parallel. We also proposed an alternative formulation of the adaptive strategy that is suitable to handle noise in the received signal and tested the strategy with respect to small mismatches in the parameters of the individual oscillators. The novelty of our approach is demonstrated by the fact that it can reconstruct the structure of an unknown complex network from dynamical information even when partial knowledge of its nodes' time evolutions is available.

A limitation is represented by the possibility of extending our approach to larger networks, which are characterized by a larger parameter search space. Though it is both possible and desirable that other methods will outperform ours in achieving this goal, we expect that being able to correctly estimate the structure of an unknown large network from limited dynamical information will remain an outstanding task, irrespective of the specific approach used. In this regard, our method based on estimating single modules of oscillators from a large network and recombining them to obtain a picture of the original network may prove useful even when alternative approaches are attempted.

ACKNOWLEDGMENTS

F.S. would like to thank Wai Lim Ku for useful comments on the identification of genetic networks. R.D. is grateful for funding from the Luce Foundation.

[1] H. D. I. Abarbanel, Daniel R. Creveling, and J. M. Jeanne, Phys. Rev. E **77**, 016208 (2008).

[2] Daniel R. Creveling, Philip E. Gill, and Henry D. I. Abarbanel, Phys. Lett. A **372**, 2640 (2008).

[3] H. D. I. Abarbanel, P. H. Bryant, P. E. Gill, M. Kostuk, J. Rofeh, Z. Singer, B. Toth, and E. Wong, in *The Dynamic Brain: An Exploration of Neuronal Variability and Its Functional Significance* (Oxford University Press, New York, 2011), p. 139.

[4] J. C. Quinn, P. H. Bryant, D. R. Creveling, S. R. Klein, and H. D. I. Abarbanel, Phys. Rev. E **80**, 016201 (2009).

[5] W. Yu, G. Chen, J. Cao, J. Lu, and U. Parlitz, Phys. Rev. E **75**, 067201 (2007).

[6] F. Sorrentino and E. Ott, Chaos **19**, 033108 (2009).
[7] F. Sorrentino, Phys. Rev. E **81**, 066218 (2010).
[8] B. A. Toth, M. Kostuk, C. D. Meliza, D. Margoliash, and H. D. I. Abarbanel, Biol. Cybern. **105**, 217 (2011).
[9] M. Kostuk, B. A. Toth, C. D. Meliza, D. Margoliash, and H. D. I. Abarbanel, Biol. Cybern. **106**, 155 (2012).
[10] S. V. Buldyrev, R. Parshani, G. Paul, H. E. Stanley, and S. Havlin, Nature **464**, 1025 (2010).
[11] R. Olfati-Saber and R. M. Murray, IEEE Trans. Autom. Contr. **49**, 1520 (2004).
[12] R. Olfati-Saber, IEEE Trans. Autom. Contr. **51**, 401 (2006).
[13] A. de la Fuente, P. Brazhnik, and P. Mendes, Trends Genet. **18**, 395 (2002).
[14] N. Friedman, Sci. Signal. **303**, 799 (2004).
[15] A. De la Fuente and D. P. Makhecha, Syst. Biol. **153**, 257 (2006).
[16] J. J. Faith, B. Hayete, J. T. Thaden, I. Mogno, J. Wierzbowski, G. Cottarel, S. Kasif, J. J. Collins, and T. S. Gardner, PLoS Biol. **5**(1), e8 (2007).
[17] D. Marbach, C. Mattiussi, and D. Floreano, Ann. NY Acad. Sci. **1158**, 234 (2009).
[18] R. De Smet and K. Marchal, Nat. Rev. Microbiol. **8**, 717 (2010).
[19] D. Marbach, R. J. Prill, T. Schaffter, C. Mattiussi, D. Floreano, and G. Stolovitzky, Proc. Nat. Acad. Sci. USA **107**, 6286 (2010).
[20] M. C. Boelens, G. J. Te Meerman, J. H. Gibcus, T. Blokzijl, H. M. Boezen, W. Timens, D. S. Postma, H. J. M. Groen, and A. Van Den Berg, BMC Genom. **8**, 277 (2007).
[21] A. Roberts, C. Trapnell, J. Donaghey, J. L. Rinn, L. Pachter, *et al.* Genome Biol. **12**, R22 (2011).
[22] J. G. White, E. Southgate, J. N. Thomson, S. Brenner, J. G. White, E. Southgate, J. N. Thomson, and S. Brenner, Philos. Trans. R. Soc. London B **314**, 1 (1986).
[23] F. Sorrentino and E. Ott, Phys. Rev. Lett. **100**, 114101 (2008).
[24] F. Sorrentino and E. Ott, Phys. Rev. E **79**, 016201 (2009).
[25] Adam B. Cohen, Bhargava Ravoori, Francesco Sorrentino, Thomas E. Murphy, Edward Ott, and Rajarshi Roy, Chaos **20**, 043142 (2010).
[26] F. Sorrentino and P. DeLellis, Chaos, Solitons & Fractals **45**(1), 35 (2011).
[27] Wenwu Yu and Jinde Cao, Chaos **16**, 023119 (2006).
[28] X. Q. Wu, Physica A **387**, 997 (2008).
[29] Hui Lui, Junan Lu, and Jinhu Lu, *IEEE International Symposium on Circuits and Systems (ISCAS 2008)* (IEEE, New York, 2008), pp. 109–112.
[30] Jin Zhou and Junan Lu, Physica A **386**, 481 (2007).
[31] D. Yu, M. Righero, and L. Kocarev, Phys. Rev. Lett. **97**, 188701 (2006).
[32] Hui Lui, Junan Lu, Jinhu Lu, and D. Hill, Automatica **45**, 1799 (2009).
[33] J. Cao and J. Lu, Chaos **16**, 013133 (2006).
[34] A. H. Cohen, S. Rossignol, and S. Grillner, *Neural Control of Rhythmic Movements in Vertebrates* (Wiley, New York, 1988).
[35] F. C. Hoppensteadt and E. M. Izhikevich, *Weakly Connected Neural Networks*, Vol. 126 (Springer-Verlag, New York, 1997).
[36] N. Kopell, in *The Handbook of Brain Theory and Neural Networks* (MIT Press, Cambridge, MA, 1998), pp. 178–183.
[37] D. R. Chialvo, Chaos Soliton. Fract. **5**, 461 (1995).
[38] M. P. K. Jampa, A. R. Sonawane, P. M. Gade, and S. Sinha, Phys. Rev. E **75**, 026215 (2007).
[39] G. Buzsáki, Neuron **68**, 362 (2010).
[40] S. L. Geffeney and M. B. Goodman, Neuron **74**, 609 (2012).
[41] O. Sporns, G. Tononi, and R. Kötter, PLoS Comput. Biol. **1**, e42 (2005).
[42] J. W. Lichtman, J. Livet, and J. R. Sanes, Nat. Rev. Neurosci. **9**, 417 (2008).
[43] H. S. Seung *et al.*, Neuron **62**, 17 (2009).
[44] M. P. van den Heuvel and O. Sporns, J. Neurosci. **31**, 15775 (2011).
[45] D. Kleinfeld, A. Bharioke, P. Blinder, D. D. Bock, K. L. Briggman, D. B. Chklovskii, W. Denk, M. Helmstaedter, J. P. Kaufhold, W. C. A. Lee *et al.*, J. Neurosci. **31**, 16125 (2011).
[46] R. Vardi, A. Wallach, E. Kopelowitz, M. Abeles, S. Marom, and I. Kanter, Europhys. Lett. **97**, 66002 (2012).